

10-23-1989

Practical Aspects of Automatic Orientation Analysis of Micrographs

N. K. Tovey
University of East Anglia

P. Smart
University of Glasgow

M. W. Hounslow
University of East Anglia

X. L. Leng
University of Glasgow

Follow this and additional works at: <https://digitalcommons.usu.edu/microscopy>

 Part of the [Biology Commons](#)

Recommended Citation

Tovey, N. K.; Smart, P.; Hounslow, M. W.; and Leng, X. L. (1989) "Practical Aspects of Automatic Orientation Analysis of Micrographs," *Scanning Microscopy*. Vol. 3 : No. 3 , Article 8.

Available at: <https://digitalcommons.usu.edu/microscopy/vol3/iss3/8>

This Article is brought to you for free and open access by the Western Dairy Center at DigitalCommons@USU. It has been accepted for inclusion in Scanning Microscopy by an authorized administrator of DigitalCommons@USU. For more information, please contact digitalcommons@usu.edu.



PRACTICAL ASPECTS OF AUTOMATIC ORIENTATION ANALYSIS OF MICROGRAPHS

N.K. Tovey⁺, P. Smart⁺⁺, M.W. Hounslow⁺, and X.L. Leng⁺⁺

⁺ School of Environmental Sciences, University of East Anglia, NORWICH NR4 7TJ.

⁺⁺Department of Civil Engineering, University of Glasgow, GLASGOW G12 8QQ.

(Received for publication March 16, 1989, and in revised form October 23, 1989)

Abstract

Techniques to analyse the orientation of particulate materials as observed in the scanning electron microscope are reviewed in this paper. Emphasis is placed on digital imaging, processing, and analysis methods, but many secondary electron images are not amenable to traditional image processing as adequate thresholding is often difficult to achieve. Evaluation of the intensity gradient at each pixel offers an alternative approach, and this method is described in detail including the latest developments to generalize the technique. Practical points in the acquisition, processing and analysis of the images are considered and several images, including both synthetically generated and actual back-scattered images of soil particle arrangements are presented. A discussion of methods to display the results is included as are possible future developments.

Key Words: Electron micrographs, particulate materials, quantitative analysis, handmapping, digital techniques, orientation analysis, intensity gradient, edge detection, anisotropy, practical tips.

*Address for Correspondence:

N. K. Tovey,
School of Environmental Sciences,
University of East Anglia,
Norwich,
NR4 7TJ,
UK.

Phone No: 0603 56161 x2550/2553

Introduction

There are many branches in Science in which a knowledge of the size, shape, and orientation of features is of importance. For instance, in particulate materials, the macroscopic properties depend on the spatial arrangements of the particles themselves both in terms of orientation and packing. Equally, in fibrous materials, many macroscopic properties will exhibit anisotropy. Optical and electron micrographs convey much information on the spatial arrangements of features, and much work has been done in recent years to develop methods to automatically process such images, and provide meaningful statistics on the constituent features.

In some disciplines, the term 'microfabric' is defined as the spatial (three-dimensional) arrangement of the constituent solid particles and their associated voids. Some disciplines also treat 'microstructure' as synonymous with 'microfabric', while others do not. In this paper the term 'microfabric' will be used throughout.

One of the problems associated with the study of microfabric has been its variability in some specimens over small distances, and subjective statements about the presence or absence of orientation in a single micrograph are difficult to reconcile with the overall situation when several micrographs must be studied. With the advent of image analysis and image processing techniques, the situation may be helped as automation of some of the analyses is now possible.

Over the last 25 years, many different methods have been investigated in an attempt to obtain quantitative parameters to describe microfabric or the degree of orientation. These in turn can then be related to external physical conditions such as stress condition, flow of water through the medium, etc. Four basically different methods have evolved:-

- i) handmapping
- ii) microphotogrammetry
- iii) optical techniques
- iv) digital techniques (image processing/analysis)

This paper will concentrate primarily on the digital techniques, consider in depth some of the practical aspects of that technique, and in particular, consider the current developments in the Intensity Gradient Techniques for orientation analysis. As such the paper will complement the recent paper by Smart and Tovey (1988) which outlined a general theory of this last method. A discussion of the hand mapping techniques is included as image processing techniques can be used to enhance certain aspects of this technique. Both microphotogrammetry and optical techniques are reviewed briefly first.

Microphotogrammetry is a separate technique and is described in Smart and Tovey (1982), where the fully general equations for the central projection case with any number of specimen tilt arrangements are included. In a simple form, stereophotographs may be used to determine the coordinates of selected points in all three dimensions. From a knowledge of this, a true three dimensional estimate of particle alignments may be made, and this is a distinct advantage of the techniques over the others described here. On the other hand the technique is extremely time consuming, although some progress towards automation has been made, and Tovey (1978) outlined how this may be done. At present, the automation extends only as far as spot height measurement or the preparation of contour maps. When the alignments of particles are needed, a further step is needed to identify the individual particles from the contour information.

Microphotogrammetric techniques only work adequately for orientation analysis where the size of the particles in the image is relatively large, and thus the magnification must be high. However, recent studies using the intensity gradient technique, described later, indicate that the variability is such that tens of micrographs are needed to get a statistically relevant assessment of particle alignments from just one sample. Since the area covered in the micrographs analysed by the intensity gradient technique are up to 25 times the area of that for photogrammetric analysis, several hundred analyses would seem necessary to achieve a reliable estimate by this means. It is partly for this reason that effort has been diverted away from the photogrammetric methods in recent years so that rapid analyses can be conducted. Once an area has been found which is (objectively) representative of the whole sample, then this is the one that is selected for detailed analysis by photogrammetry.

Optical techniques to examine fabric in an SEM were first used by Tovey (1971) as a means to attempt to provide the necessary rapid assessment mentioned above. These techniques involve the generation of optical transform patterns or convolution square patterns from transparencies of the image. The patterns generated from aligned fabrics show distributions of diffraction maxima spaced asymmetrically around the central maximum. The overall shape of this pattern may relate to the mean alignment of the features in the image, and some success was obtained by subjectively outlining the overall pattern which approximated to an ellipse in most cases. The

ratio of the lengths of the principal axes of this ellipse was used to quantitatively describe anisotropy of the fabric. While this technique showed some promise, the subjectivity involved in defining the overall pattern shape was a limiting factor, particularly since the intensity gradient technique can achieve the same result objectively. A further problem has been that it was often desirable to determine the magnitude of the diffraction maxima, something which is not easy from the photographic recording medium.

Despite this limitation it is likely that the equivalent technique, the digital generation of fast Fourier transforms using image processing techniques will in the future, provide a renewed interest in the technique as magnitude information will be directly available.

Hand mapping

Some of the earliest attempts at fabric quantification derived from hand mapping methods (e.g., Smart 1966, McConnachie 1974). In these, an area of an image showing a broadly similar microfabric or orientation was outlined on the micrograph. Other areas of the image showing different orientation or microfabric are outlined separately. The technique is most suitable for examination or classification of two dimensional images such as transmission electron micrographs. It is less useful for high magnification secondary electron micrographs, but the advent of high resolution back-scattered images now means that these micrographs can also be treated in a similar way.

The discrimination between the different areas is somewhat subjective, but such techniques do represent an important step forward in attempting to relate microscopic features to macroscopic properties. In early work, the areas defined in the hand mapping were measured using a planimeter, or by cutting out the separate areas and weighing them. In this way the proportion of fabric of one type, or the proportion of the sample covered with features aligned in a particular direction could be evaluated.

One difficulty of the hand mapping technique is that only broad classifications of orientation can be specified, and indeed much of the early work used just four basic classes (see for example Fig.1.40 in Smart and Tovey (1982)). These were areas in which the particles were aligned approximately vertical, horizontal, 45° upwards to the right, or 45° upwards to the left. A fifth category specifying an area in which there was no preferred orientation was included. By estimating the proportion of the areas aligned in the four directions it is possible to ascertain whether any overall preferred orientation exists within the sample, and if so by how much. One difficulty here, of course, arises when the four orientation classes are present in almost equal proportions. In theory, it should be possible to automatically evaluate the orientation of features using image analysis, and thereby remove the initial subjective demarcation. This topic is covered at length later in the paper.

Other applications of hand mapping include the allocation of areas of similar microfabrics where orientation itself is of less importance compared to other attributes such as the range of particle sizes and their aggregation within a particular area. This is a pattern recognition problem and automation of this aspect is still some distance away.

Future development of the hand mapping technique could involve the outline sketching of the different areas using a 'mouse', and then computing these areas using standard image analysis techniques. Thus an area containing particles aligned generally in one direction could be outlined, and this shape used as the mask to set the intensity within the area to a predetermined value. All other areas in the image could be treated in a similar manner, and also coded with the same intensity level. Areas with different alignments are then treated similarly, but the areas are 'painted' with a separate intensity level. When the whole image is so coded, a histogram of intensities covering the selected range may then be computed, and this will give the proportion of each separate orientation type in the image as a whole.

Currently the authors are using a scheme where the intensity level of the original image goes from 0 (black) to 239 (white), as most images do not cover the full 255 grey levels anyway. In those images where there is full coverage, a simple rescaling of the range to 0-239 will suffice. By doing this, the intensity values 240-255 may be used to define separately defined areas. The look up table used in this analysis is a false colour one in which there is a true grey scale (0-239) followed by discrete colours for each of the intensity values 240 to 255. In this way the image is slowly coloured with different colours as the analysis progresses, while the original image remains as an easily understood monochrome image.

The above approach is currently of use for assessing orientation patterns, particularly for those who lack the full range of image analysis facilities. However, much of the subjective assessment in delineating areas of similar orientation may be overcome using the digital techniques now available, such as the intensity gradient technique.

On the other hand, for the more general hand mapping of different classes of microfabric, based on pattern recognition rather than orientation, an enhanced hand mapping technique such as the one described above can assist considerably in quantitatively describing fabric. Image analysers work conveniently by comparing or processing different intensity levels. In problems involving pattern recognition, it is not intensity changes as such which are relevant, but the groupings the features make. The human eye can be very efficient at identifying patterns of similar type, and by outlining such areas, and setting the whole enclosed areas to fixed intensity values, the image can be readily transformed into one which can be processed by the image analyser to produce the relative distribution of fabrics of a given type. It would seem that this is an important improvement,

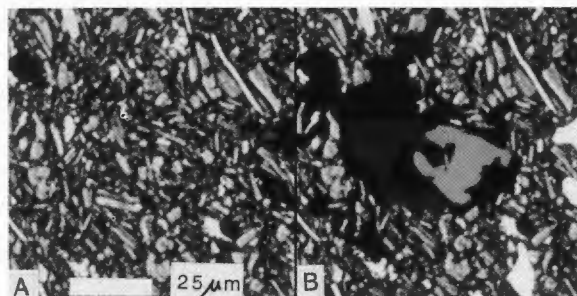


Fig. 1. Example of handmapping to delineated features of similar texture. Fig. 1A, original micrograph. Fig. 1B, some areas of similar structure have been electronically 'painted' in a fixed grey level. False colour representations provide clearer patterns than are possible here.

at least until fully automatic pattern recognition becomes a reality. Fig. 1 illustrates this technique. Fig. 1A shows the original image, and Fig. 1B shows the same area with some areas 'painted in'. In the monochrome representation here it is not possible to demonstrate the full effect when false colour is available, as in practice, many more separate colours may be used than can be shown as distinctly separate grey levels in Fig. 1B.

Digital Techniques - Introduction

The recent development of image analysers has generated much interest in the possibility of processing scanning electron micrograph images. There are basically three aspects to this:-

1) The acquisition of the image in digital form. This may be achieved by producing a transparency or print, grabbing the image via a camera or densitometer attached to an image processor and stored in digital form for subsequent processing. Alternatively, the signal may be digitized directly from the scanning electron microscope analogue signal.

2) The processing of the acquired image into a form suitable for analysis. This may be to enhance contrast, highlight specific features, filter noisy pictures, threshold images, or create binary representations. This may well involve considerable operator input when there are difficult images to process.

3) The analysis of the processed image to obtain statistical data about the image or compute parameters which may be related to the macroscopic conditions of the specimen. In addition, this aspect covers the selective measurement of a few features directly on the screen.

In theory, all three of the above aspects could be attached directly to an SEM. However, unless all three are highly automated and image processing and analysis take place at near real time speeds problems could arise. In the processing aspect, time may well be needed to achieve the required binary image for instance.

During this time, the SEM is effectively not usable by others, and in organisations where there is pressure to use such instruments, such operations are not an effective use of resources. It may well be appropriate to store the image on a floppy disk or other medium directly in step (1), and then transfer the digitized image to a separate image analyser. On the other hand, where powerful near real time processors are available, and operator intervention at the processing stage is not needed, there will be advantages if direct on-line facilities exist. Here the data may be processed directly without the need to permanently store or record images.

The present authors currently acquire digital images from both a Hitachi S-450 and a Hitachi S-800 scanning electron microscope, both of which are equipped with back-scattered detectors. The image processing and analysis is done on a microcomputer using the Synoptics SEMPER 6 software which has been extended to incorporate the facilities described in this paper. Much of the work described here relates to image analysis and only limited reference is made to image processing.

Traditional Methods Of Orientation Analysis

Much of the recent interest in image processing and analysis has involved the enhancement/filtering of images, the selection of a suitable threshold to transform the image into a binary form, and the processing to determine particle statistics such as shape, size, orientation, etc. Many software packages are available for such analysis, and most image analysers have such features as standard. However, a key aspect of this approach is the ability to correctly threshold an image. In some types of image this may be a little problem, but where the background varies from region to region, this may create a major obstacle to full automation of the procedure as each image must be suitably processed before analysis. This can be very time consuming and difficult to achieve adequately if the background intensity varies greatly as it often does in many secondary electron images.

Fig. 2 shows an image taken from a scanning electron microscope of some spherical latex particles. The requirement of most particle statistics facilities is that the image is transformed by a stepwise intensity transform where each step represents a separate feature. In the basic form of this, the original image is transformed into a binary image where one intensity represents the particles and another the voids. Once in this form the normal routines can readily provide all the particle statistics that can ever be needed such as size, shape, perimeter, orientation, circularity, etc. The acquisition of a binary image from a secondary electron image such as that in Fig. 2 can cause problems. For example, subjective observation clearly identifies the individual particles; but successive binary images with the thresholds moved by just 1 grey level fail to adequately discriminate the particles from the background.

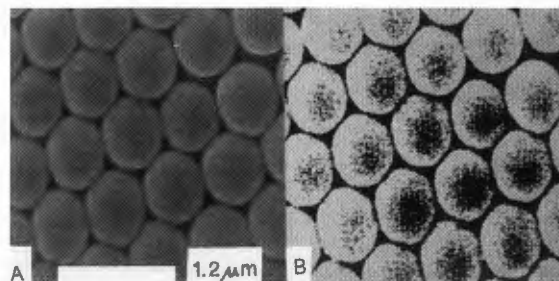


Fig. 2. Example to highlight problem of thresholding. Fig. 2A shows a secondary electron micrograph of latex spheres. Fig. 2B shows the best binary image that can be obtained without pre-processing. The dark areas within the particles can cause difficulties in subsequent analysis unless they are suitably filtered or masked.

Part of the problem lies in the variation in intensity across each particle, and also a general variation across the image as a whole.

Three obstacles to normal images analysis exist in such an image. Firstly, some particles remain joined even though the eye can detect the edges. Secondly, there can be 'holes' or dark areas appearing as artefacts in the centre of particles in binary images. Thirdly, small spurious particles may appear as noise. The last group may be removed using erosion/dilation techniques, by specifying a minimum area of particle to be analysed, or by masking a spurious feature for deletion. The joining of particles can be overcome by 'drawing' lines on the screen with the 'mouse' or cursor keys, and finally, the holes can be filled by using a suitable masking function. An alternative approach would be to use back-scattered images when topographic variations on each particle will be minimized and discrimination will be largely on the basis of composition. Suitable choice of the background medium to enhance the chemical contrast can also help here, although the problem of joining particles is likely to be more acute. Much separation by manual means may be necessary if adequate dispersion of the particles cannot be achieved in the first place.

All three image processing stages above can require considerable operator intervention. Some progress towards automation is possible. For instance, a predetermined number of cycles of erosion and dilation could be included. Alternatively, intensity ramp removal to even the mean intensity across an image may be possible, or even smoothing of the image followed by edge filtering and thinning to suppress small variation in the background or the particles, but enhance the major edges. However, experience shows that although it may be possible to define a suitable technique for a particular sample, separate procedures must be defined for each

different type of sample. In any case, not all image analysers permit significant user written software to be included. It would also appear unwise to allow a fully processed image to proceed to particle analysis without a check by the operator.

Once a suitable binary image has been obtained, processing and analysis is relatively straight forward. Many techniques have been suggested for analysis including some novel ones such as, Ehrlich et al (1984) and Ehrlich and Crabtree (1989) who have used successive erosion/dilation cycles to classify pore shapes and sizes in rocks.

An alternative approach involving the discrimination of edges by examining intensity gradients as a means to assess orientation patterns has been less frequently used, partly because most image analysers which do provide facilities do so with primitive algorithms. While many workers have suggested edge detection algorithms such as Marr and Hildreth (1980), Haralick (1984), and Zhou et al (1989), these have been developed primarily for edge detection and not for orientation analysis as described in this paper. In edge detection methods, and the intensity gradient technique in particular, it is the changes in intensity which are important and it is usually not necessary to do any processing before the analysis. Since absolute values of intensity are not required, the problems of thresholding do not arise, and direct image analysis with little or no intervening processing is possible. A further advantage is that the orientation of features evaluated by this method is directly related to the size and shape of a feature, rather than the specification of a single orientation given by the more normal methods.

The Intensity Gradient Technique

While developing on-line image processing facilities for an SEM, Unitt (1976) realized that a digital intensity gradient evaluation would provide orientation data about features in the image. He demonstrated the technique using a digitized version of a micrograph of one of the present authors (NKT). While some image analysis facilities do have as standard a function to evaluate the intensity gradient, they in general, do not provide algorithms of sufficient precision for reliable orientation analysis. Several separate aspects of the intensity gradient technique are considered in this paper. First, a review of the historical development, secondly, new theoretical developments, thirdly, practical points on the technique, and finally, presentation of the results.

In its most simple form, the intensity gradient technique for orientation analysis considers the rate at which the intensity is changing in two orthogonal directions across a micrograph. If there is a linear feature in the micrograph, then this intensity will vary in a direction orthogonal to the alignment of that feature, and this is readily evaluated once the intensity gradient is known in the two orthogonal directions.

By evaluating this intensity gradient vector at every point within an image a measure of the overall orientation of features in the field of view may be obtained.

Fig. 3 shows a numbering arrangement of 24 pixels surrounding a pixel of interest. The numbering scheme has been specifically chosen for efficient use in the analysis. If I_n is the intensity at the nth point, then the intensity gradient in the x - direction is given by:-

$$\frac{\delta I}{\delta x} = \frac{I_1 - I_0}{h} \quad (1)$$

where h is the spacing between pixels.

A similar expression may be formulated for $\delta I/\delta y$ involving points 2 and 0.

Finally, the direction of the intensity gradient vector (i.e., the one specifying the direction of greatest change of intensity) is given by:-

$$\tan \theta = \frac{\delta I/\delta y}{\delta I/\delta x} \quad (2)$$

which in this particular situation will be:-

$$\tan \theta = \left\{ \frac{I_2 - I_0}{I_1 - I_0} \right\} \quad (3)$$

while the magnitude of the vector V_I is:-

$$V_I = \sqrt{\left(\frac{\delta I}{\delta x}\right)^2 + \left(\frac{\delta I}{\delta y}\right)^2} \quad (4)$$

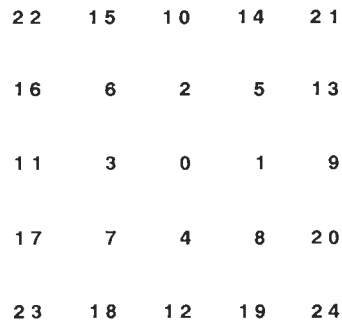


Fig. 3. Numbering arrangement for pixels used in intensity gradient technique. The numbers are arranged for convenience in using the general methods.

Unitt (1975, 1976) and Unitt and Smith (1976) were the first to derive intensity gradient relationships and apply them to scanning electron microscopy. In their analysis, they extended the algorithm to include points 3 and 4 to derive formulae for what later became known as the 5 - point method. Unitt (1976) realized that this latter method was prone to the limited range of values (integer values 0 to 255) that the intensity at any one point may take. When variations in intensity were small, the difference functions in both the numerator and

denominator are also small, and thus only a few values of θ are possible. This is particularly noticeable when a rosette histogram of angles is plotted. Spikes on the rosette diagram highlight the preferentially selected angles (Tovey and Smart (1986)).

In an attempt to overcome this, Unitt (1976) extended the analysis to include points 1-4 and 9-12 in what later became known as the 9C - point analysis. This extended method improved matters, but Tovey (1980) showed that problems still arose with regions where the intensity varied little, and suggested that vectors with a magnitude less than $2.0/h$ should be omitted in the aggregation of results to form a rosette diagram. Indeed he considered also displaying rosette diagrams for different ranges of magnitude.

The exclusion of vectors of low magnitude was studied in much greater detail by Tovey and Smart (1986) when it was shown that provided class widths in the rosette diagram of 5° were chosen, that there was justification for choosing the threshold at a magnitude of $2.0/h$. In that paper Tovey and Smart showed rosette diagrams for the orientation of vectors with low magnitude - the very ones which it was proposed should be excluded. The resulting low magnitude diagrams from three very different images were similar to each other. On the other hand, the corresponding diagrams for vectors of higher magnitude were very different. A further pertinent point was that the low magnitude rosette diagrams were also almost identical with those generated in a random computer simulation.

Tovey and Smart (1986) also considered two other groupings of points, namely points 1-8 inclusive (known as the 9S - point method), and also an arrangement with points 1-12 and 21-24 included (17 - point method). Despite its apparently better shape, the 9S - point method proved to be inferior to the 9C - point method, although the 17 - point method proved superior, albeit with some time penalty in computation.

Apart from specifically excluding the vectors of low magnitude in deriving the rosette diagrams, little specific application has been made of the selection of different ranges of magnitude. In most cases, the aggregate diagram has been evaluated, but recently, Tovey and Krinsley (submitted for publication) have shown that specific ranges of magnitudes may be used to highlight certain effects. For instance, in basaltic samples they noted a characteristic pattern in the diagrams of magnitude range $2.0/h$ to $5.0/h$. Equally, specific orientation directions were seen on sand grains. The choice of ranges used was somewhat arbitrary, and there is clearly reason to investigate the distribution of vectors in different magnitude classes.

Recent Theoretical Developments In Intensity Gradient Analysis.

Apart from the equations derived above four separate formulae have been derived for each of $\delta I/\delta x$ and $\delta I/\delta y$ corresponding to the four methods described in Tovey and Smart (1986). In a recent paper Smart and Tovey (1988) derived a fully general method which is valid for all groupings

of points in Fig. 3, and yet requires the once and for all derivation of a set of equations. The full theoretical derivation is given in the above paper, and for the purposes of the present paper the following is sufficient.

The intensity (I_p) of a pixel P which is at a distance h in the x - direction from the central pixel O may be expressed as an expansion of Taylor's theorem:-

$$I_h = I_0 + h \frac{dI}{dx} + \frac{h^2}{2!} \frac{d^2I}{dx^2} + \frac{h^3}{3!} \frac{d^3I}{dx^3} + \dots \quad (5)$$

using D to represent $\frac{d}{dx}$ equation (5) may be represented by:-

$$I_h = I_0(1 + hD + \frac{h^2 D^2}{2!} + \frac{h^3 D^3}{3!} + \dots) \quad (6)$$

and this reduces to $I_h = e^{hD} I_0$ (7)

In two dimensions, the substitutions:-

$$D_x = \frac{\partial}{\partial x} \qquad D_y = \frac{\partial}{\partial y}$$

may be used and the relevant two dimensional equation becomes:-

$$I_h = e^{h_x D_x} . e^{h_y D_y} . I_0 \quad (8)$$

where h_x and h_y are the pixel spacings parallel to the x - and y - directions, respectively.

The full expansion of equation (8) gives two terms of the first order, three terms of the second order, four of the third, and five of the fourth order and so on. Excluding the unity constant there are thus two terms up to and including the first order, five up to the second order, and 9, 14, and 20 up to and including the third, fourth and fifth orders respectively. Thus the third order terms include the term:-

$$\frac{1}{2} . h_x^2 h_y D_x^2 D_y,$$

while the fifth order terms include the term:-

$$\frac{1}{12} . h_x^3 h_y^2 D_x^3 D_y^2,$$

and a separate equation may be written for each pixel depending on the values of h_x and h_y at that pixel.

In the evaluation of the intensity gradient it is the quantities D_x and D_y which must be evaluated, and all other terms such as $D_x^n D_y^m$ must be eliminated. To do this the coefficients $h_x^n h_y^m$ must be determined. At the point 24 in Fig. 3, $h_x = 2$ and $h_y = 2$, the coefficient $h_x^3 h_y^2$ becomes $2^3 . (-2)^2 = 32$. Equally, the coefficients at the points 14 and 16 become 4 and -8,

respectively.

These coefficients need to be evaluated only once. Thus for a first order equation there are two terms, one for D_x and one for D_y , and 24 pairs of coefficients each one for a different pixel in the array in Fig. 3. A 2×24 matrix of coefficients may thus be constructed to represent the situation. Including terms of the second order requires a 5×24 matrix, while if all terms up to and including the fifth order are included a 20×24 array of coefficients must be determined. The full matrix of coefficients is displayed in Smart and Tovey (1988) as Table II. In theory there is no reason why the matrix should not be extended further to include all points in a 7×7 pixel array or even larger, and in such cases higher order solutions would be possible.

If the coefficients of the derived matrix are b_{ij} , and the 20 expressions of the form:-

$$I_i - I_0 = \sum_{j=1}^{20} b_{ij} D_x^m D_y^n$$

are replaced by the column vector \mathbf{X} , then the series of equations for the different points may be reduced to:-

$$\mathbf{B} \cdot \mathbf{X} = \mathbf{C} \quad (9)$$

where \mathbf{C} is the column vector containing terms of the intensity difference between the i th point and the pixel 0 (i.e. $I_i - I_0$).

For any given value of i , the exact value of a coefficient b_{ij} depends on the order in which the coefficients in \mathbf{X} are arranged, but a convenient arrangement is to have the two first order terms (D_x and D_y) represented by X_1 and X_2 , respectively. The three second order terms are then represented by $X_3 - X_5$. Once the order has been fixed, it is only necessary to evaluate the coefficients once, and thereafter, the relevant sub-matrix may be extracted from the full 20×24 matrix to provide the necessary set of coefficients for evaluation of the intensity gradient vector.

The nomenclature used in the analysis now takes the form \mathbf{S}, \mathbf{T} where \mathbf{S} represents the number of pixels included in the analysis, and \mathbf{T} represents the number of differential coefficients included. Thus a $20, 14$ analysis uses points 1 - 20 to solve for the 14 coefficients needed for a fourth order solution. Clearly only 14 points are needed for such analysis, and a $20, 14$ analysis is overdetermined. This can readily be handled using normal statistical methods, such that:-

$$\mathbf{X} = \mathbf{A}^{-1} \cdot \mathbf{B}^T \mathbf{C} = \mathbf{E} \cdot \mathbf{C} \quad (10)$$

where $\mathbf{A} = \mathbf{B}^T \cdot \mathbf{B}$
and $\mathbf{E} = \mathbf{A}^{-1} \cdot \mathbf{B}^T$

Once X_1 and X_2 are known from equation (10), they can be substituted into equations (2) and (4) to derive the direction and magnitude of the intensity gradient vector. Only the first two rows of the matrix \mathbf{E} are needed, and these

rows separately represent the coefficients of two 5×5 masks by which the relevant pixels in the image must be multiplied in order to obtain D_x and D_y .

Practical Points

The equations above have been derived assuming that the pixels are square, although Smart and Tovey (1988) did also consider the case with rectangular pixel image stores. Clearly, some care must be taken to ascertain the shape of the pixels in the frame store on both the image analyser and the SEM. Thus though the image analyser used by the authors does indeed have square pixels, the frame grabbing facilities on one of their scanning electron microscopes has rectangular pixels. Most scanning electron microscopes are provided with a tilt compensator, which effectively adjusts the area scanned on the specimen to compensate for foreshortening effects. In the past, this control has been of dubious value as it only corrects for tilt distortion if parallel projection conditions prevail (i.e. magnifications greater than $\times 1000$), and the topographic relief is very small. In cases where the topographic relief is large, the use of such a control introduces other distortions, and should thus be avoided. However, if as is usual for image analysis, the specimen is observed at 0° tilt, then the tilt compensation may be used not to compensate for tilt, but to adjust the scan in the 'Y' direction to compensate for the rectangular pixel array.

The full combination of SEM and image analyser must be calibrated using a standard grid to ensure that the images to be analysed will be processed in the correct form. Indeed such calibration is also essential to provide the calibration constant between pixel size and real dimensions in the SEM, and applies to both the intensity gradient technique and also the more traditional particle analysis outlined earlier.

Equation (2) will produce angles in the range $0 - 360^\circ$, but in practice only angles between 0 and 180° are needed as a vector representing a rod shaped particle or the normal to a planar particle may point in either of two opposite directions. It is convenient for many purposes to select the direction which falls between 0 and 180° . While it is convenient to represent particles by the vector normal, in most situations arising from two dimensional images, this vector normal is at right angles to the long axis of particles. Experience has shown that in two dimensional images confusion is often caused by expressing vectors in this manner, and the present authors now prefer to display the vectors which will coincide with the long axis of the feature

In theory there would appear to be a large number of possible methods of analysis for each value of \mathbf{S} and \mathbf{T} , but the situation is simplified considerably, since for a given order solution all derivatives up to and including that order must be included. Thus \mathbf{T} can only take the values 2, 5, 9, 14, and 20 in a 5×5 array. Similarly, it will be normal practice to use only symmetric arrays, and so in these cases, \mathbf{S} can

only take the values 4, 8, 12, 20, and 24.

Examples of the coefficients for selected **S, T** methods from the first row of **E**, i.e. relating to D_x , are shown in Smart and Tovey (1988 for the **20,14** and **12,9** methods) and Tovey et al (1989 for the **24,14** method). Two possibilities exist for application of this general technique in practice.

In one possibility, the coefficients of **E** for any one **S, T** method need only be evaluated once for any pixel numbering arrangement. Thereafter, these coefficients could be stored in a permanent data array in any program. Equally several different sets of coefficients may be stored each one corresponding to one of the selected values of **S** and **T** above. This gives flexibility of choice as to the precision of the analysis. It is found that certain pairs of **S, T** methods have identical coefficients which would reduce the storage space significantly. Thus the **20,14** and **20,9** methods have identical coefficients, while the **8,5** and **8,2** methods form another pair. Other pairings include the **12,5/12,2**, **24,14/24,9**, **24,5/24,2**, and **20,5/20,2** methods.

Since several of the coefficients are zero in many regularly used methods, specific formulae for each may be written to reduce computation time. A particular example here is the **12,9** method which is identical with the former **9C** - point method. In this method, the coefficients at points 13-24 are obviously zero, but it also turns out that the coefficients at points 5-8 are also zero. A specifically written formula is clearly more efficient here.

The second possibility for practical use is to retain the master 20×24 matrix and to evaluate the coefficients of **E** at the start of an analysis by selecting the appropriate sub-matrix from the master matrix. In this way any number of asymmetric arrays may also be included in the analysis. Here though, the full cross correlation function of the mask of coefficients with the image at every pixel will need to be evaluated. This second approach is useful where analyses different from the standard ones are required.

The normal symmetric arrays work adequately over the whole region except when the pixel 0 is less than two pixels from a boundary. In all previous work, no attempts have been made to estimate the intensity gradient within two pixels of any border, and thus the resulting number of estimates of the intensity gradient vector is $(m-2) \times (n-2)$ for an image m pixels wide by n pixels deep. An extension to the analysis could use asymmetric arrays at the border. Thus an analysis using just the points 1, 2, 3, 5, 6, 9, 10, 11, 13, 14, 15, 16, 21, and 22 could be used if the bottom edge of the image passed through the pixels 11, 3, 0, 1, and 9. In this case, there are 14 pixels, and thus a fourth order solution (requiring solution to 14 separate equations) is just possible. Equally if pixel 0 is at the corner of an image, then pixels 1, 2, 5, 9, 10, 13, 14, and 21 may be used in a second order solution to estimate the intensity gradient vector at a corner. In this case there would also be some redundancy of data, and a least

squares solution is possible as outlined in equation (10) above.

In early work using the intensity gradient technique it was standard practice to generate the necessary histogram data as the intensity gradient vector was evaluated successively at every pixel. In this way it avoided the creation of two large arrays each one the dimension of the original image, and one relating to the individual angles, and the other to the corresponding magnitudes. This was of importance when storage space was at a premium, but the penalty here was that a pre-selection of histogram class widths, and also magnitude ranges was necessary. It was generally found that class widths of 5° were convenient and corresponded to the threshold criteria studied by Tovey and Smart (1986). Magnitude ranges were often chosen somewhat arbitrarily although the following ranges were often used:-

0 - 2/h, 2/h - 5/h, 5/h - 8/h, 8/h - 12/h, 12/h - 20/h, 20/h - 50/h, 50/h - 100/h.

In addition an aggregate range (excluding 0 - 2/h) was included in analyses.

A typical image 512×512 pixels requires 250 k bytes of storage if the intensity levels are represented in 0 - 255 grey levels. It is possible to store all the resulting vector directions and magnitudes as two separate images. If the resulting directions are specified to the nearest whole degree, then intensity levels 0 - 179 (or 1 - 180) may be used to store the relevant directional information. This is convenient because this leaves room to store problem situations at say a magnitude of 255. Such a case occurs where the intensity is constant over the 5×5 array when both $\delta I/\delta x$ and $\delta I/\delta y$ are zero, and the direction is obviously indeterminate. Equally, if vectors of a low magnitude are excluded, then these too can be set to this value or alternatively allocated a separate grey level value between 181 and 255.

The magnitude of the intensity gradient vector can also be stored in a separate 8-bit image. Using this approach for intensity gradient analysis instead of the previous histogram approach, greatly increases the storage requirement for a single image, but it does considerably increase the flexibility for subsequent statistical analysis. Thus the data from the two new 'images' can be combined to generate rosette diagrams for any range of magnitudes rather than just predetermined values.

With the increase in complexity of the analyses, computational time becomes important, and care must be taken to minimize unnecessary overheads. Thus reading and writing images in binary form is clearly preferable to input/output in ASCII form. Equally, certain functions needed in the intensity gradient technique are particularly time consuming to execute compared to most other functions. Two such functions which according to equations (2) and (4) must be evaluated at each pixel are 'square root' and 'arctan'.

Exact precision in the computing of the arctan function is not needed as angular values

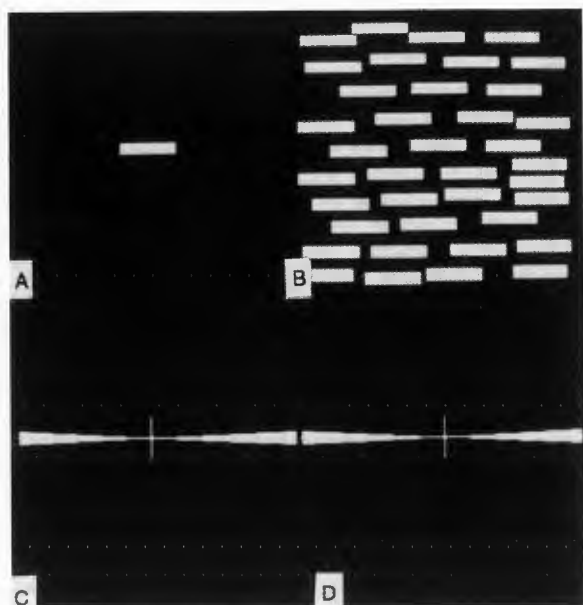


Fig. 4. A representation of a single particle (Fig. 4A) and several similarly shaped, irregularly spaced, parallel particles (Fig. 4B). The respective rosette diagrams (Figs. 4C and 4D) are identical and the ratio of the dimensions in these diagrams equals that of the individual particles.

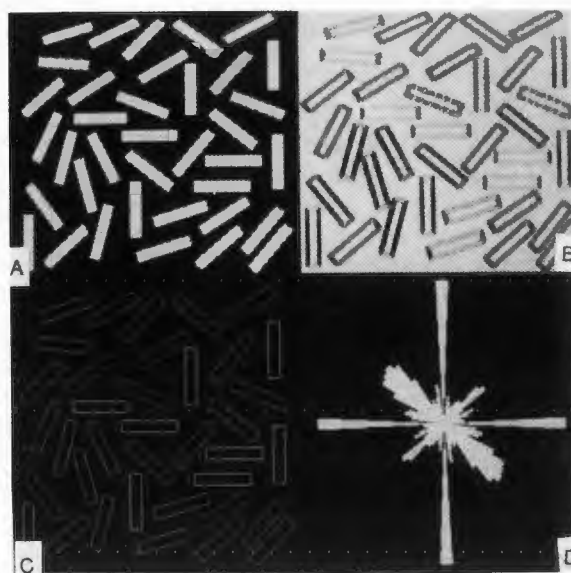


Fig. 5. A collection of randomly orientated but otherwise identical particles. (Fig. 5A) and the results of analysis using the intensity gradient technique (Figs. 5B - 5D). Fig. 5B shows the angular information where each shade of grey (ideally a separate colour) relates to a particular group of angles. Fig. 5C shows the magnitudes of the vectors illustrating how the edges are highlighted, and Fig. 5D, the associated rosette diagram.

to the nearest degree are sufficient, and an adequate accuracy may be achieved by using a look up table. This approximation may reduce the computation time significantly. The 'square root' function is needed only to compute the magnitude, and in the basic form of analysis only a threshold value of magnitude must be specified. There is no reason why this should not be specified as the square of the magnitude. Indeed, for the more general application, the magnitude data could be stored as the square function, and only converted at a later date if absolutely necessary. To achieve this it will now be necessary to store the values in 16-bit format representing the grey levels 0 - 65535. A further reduction in computing time is possible using this approach.

While the intensity gradient technique may be used at any magnification it is important to select the effective magnification so that the features of particular interest are at least 1 pixel wide. Thus with Kaolin particles $0.2\mu\text{m}$ thick, the minimum magnification to resolve such detail for intensity gradient purposes must be such that the effective pixel spacing is no greater than $0.2\mu\text{m}$. If the image covers an area $100\text{mm} \times 100\text{mm}$, and the digitized image is composed of 500 lines, then each pixel is 0.2mm square, and the required minimum magnification is $\times 1000$. Fortunately this is well within the ability to see embedded particles of Kaolin in the back scattered mode of operation.

Examples Of Simple Features

Some examples of the intensity gradient technique as applied to simple patterns are shown in Figs. 4 and 5. Fig. 4A shows a single rectangular particle while 4B shows a collection of identical particles arranged in a parallel manner. The associated rosette diagrams (Fig. 4C and 4D) are identical, and the relative ratios of the nodes in the distribution reflects the mean particle shape. Where the shape and the size of the particles vary, then provided the features are still parallel the overall shape of the rosette diagram will still indicate the mean shape of the particles.

Fig. 5A. shows an arrangement of identical particles to those in Fig 4, but this time arranged at random. Fig. 5B shows the angular data where the intensity at each pixel relates to the orientation at that pixel. The grey scale goes from black at 0° to nearly white at 180° . Regions of no contrast, where the intensity gradient vector is indeterminate, are shown fully white. On a monochrome representation such as this it is difficult to adequately discriminate between the angles, and a four grey level stepwise contrast has been used. In some cases a mottled edge to a particle appears where the angle is just at the boundary between one contrast level and another. Normally, of course, a false colour representation permits a greater

number of class levels. Fig. 5C shows the corresponding magnitude values at each pixel and clearly indicates how the edges of the particles have been highlighted. Once again a false colour representation makes the display easier to follow, but in this representation, black corresponds to a magnitude of 0 and white to magnitudes of 255.

Subsequent Analysis

As indicated above, the intensity gradient vector may be used to highlight edges of features, and this may be an alternative approach to the adaptive thresholding normally used as a preliminary processing system in image analysis systems to evaluate particle statistics. Some filtering may be needed, or alternatively the angular data image may be combined with some thresholding to produce a binary image suitable for the more usual particle analysis routines. Zhou et al (1989) have recently used an edge detection system combined with line-linking for edge tracing in the reconstruction of linear features in photographs as a step towards pattern recognition.

In general, however, where the primary purpose for doing the work has been to assess the degree of alignment, some further processing is necessary to bring the results from the raw form as angular and magnitude data images into a suitable form for analysis. Both graphical distributions and numerical estimates of orientation are needed to relate fabric patterns to macroscopic properties. Hitherto, a convenient graphical display has been the construction of a rosette histogram, in which all vectors in a given magnitude range, or as a whole for aggregate results are treated equally as unit vectors. There may well be applications where the vectors are weighted according to some function of their magnitude. This is possible where both the direction and magnitude of every vector is stored. In such situations, vectors representing 'sharp' edges to features would be weighted more heavily than 'soft' edges. This approach is an extension of that used by Tovey and Krinsley (submitted for publication). Clearly some experimentation is needed here to ascertain the correct function. A simple linear multiplier proportional to magnitude would seem inappropriate as it would unduly emphasize features from very contrasting regions. On the other hand, some weighting to include all vectors may be an alternative to the rejection of vectors of low magnitude.

The presentation of orientation patterns as a rosette diagram gives a clear indication of the proportion of features aligned in any particular direction, but in many cases a single quantitative figure is needed to describe an index of anisotropy. One way by which this may be done is to estimate the best fitting ellipse to the distribution, and express the index of anisotropy as a function of the lengths of the principal axes of this ellipse. Here there are several methods by which this index may be specified. Four possible formulae have been considered:-

i) The ratio of the length of the major principal axis to that of the minor one. This is the method used previously by the authors, and takes a value of 1.0 for a truly random fabric, and increases as the degree of orientation increases. One problem with this method is that perfect orientation of infinitely thin long features would be infinity. On the other hand the maximum value of the index for real features of similar shape and size which are parallel will approach the shape of a single feature. For parallel features of differing size and shape, the maximum index would equal the mean shape of the particles. This may be a reason for retaining this definition.

ii) The ratio of the minor axis to the major axis, or in fact the reciprocal of (i). In this case the index varies from 1.0 at random to zero for a perfectly aligned feature, and thus has finite bounds. Intuitively this is less than satisfactory as an increase in index with alignment would be preferable.

iii) A ratio expressed as:-

$$\frac{\text{major axis} - \text{minor axis}}{\text{major axis}}$$

This expression has the advantage that the index increases from zero for a random specimen to 1.0 for perfect orientation, and is the method now generally preferred by the present authors for intensity gradient analysis. It is also equal to subtracting the value obtained in (ii) above from unity.

iv) A ratio expressed as:-

$$\frac{\text{major axis} - \text{minor axis}}{\text{major axis} + \text{minor axis}}$$

This expression has been used in optical microscopic descriptions of orientation patterns, but would appear less satisfactory for the work reported here.

In all the above definitions, the direction of preferred orientation is given by the orientation of the major principal axis. A variation of the method generating a best fitting ellipse, is to weight the individual vectors by some function of their magnitude before the rosette diagrams are plotted and the equations of the ellipses evaluated. In such circumstances, greater prominence will be given to vectors of high magnitude.

While the index of anisotropy is a convenient way to describe alignment, the full equation of the ellipse is also useful, as it should permit relationships to be made with the variations in the magnitudes of macroscopic properties with direction to be more fully understood.

While many rosette diagrams do indeed approximate to an ellipse, there are situations where the approximation to an ellipse is not so helpful. Such a case arises when there are two separate preferred orientation directions each with a high degree of alignment. The rosette diagram in this case would resemble a cruciform

with the angle between the arms of the cruciform representing the mean angle between the two orientation directions. In these cases, the normalized resultant vector may be evaluated to describe the anisotropy. This is described in detail by Curray (1956) and Mardia (1972). In this the directional angles are multiplied by a factor 2 before the resultant vector is determined. At the end the angle of the resultant vector is halved.

The mean resultant length suggested by Mardia (1972) in its basic form without weighting (i.e. all the vectors are of unit magnitude), is normalized by dividing by the number of vectors when the magnitude of this vector will range from 0.0 for a random fabric to 1.0 for a perfectly orientated fabric. This normalized mean resultant length may be used as an alternative to the indices above. If a weighting of the vectors as a function of the computed magnitude is required, this can be accommodated by preceeding as above but dividing the result by the sum of the magnitudes of the original vectors. A resultant vector in this form may be more useful for relating fabric to external properties when the distributions depart strongly from a quasi elliptical form. It is also more amenable to statistical treatment as the variance of the orientations of the various vectors may be readily tested.

While indices of anisotropy or resultant vectors may be derived for individual images, the data from several images may also be combined directly in an overall histogram using either weighted or unweighted vectors as appropriate. With such overall indices the microfabric may be related to external bulk properties. One of the first cases where this was done is reported in Tovey (1989) where a trend towards increasing particle alignment with confining pressure was noted in some marine sediments from Hong Kong.

Applications Of The Technique

The intensity gradient technique may be used to study orientation patterns in electron micrographs. Particulate materials such as soils and sediments are frequently prepared as fractured or peeled surfaces and observed in the secondary electron mode. Provided that the magnification is not large and the specimen is viewed normally, the technique may be used to obtain quantitative information on alignments. A quasi two dimensional analysis is achieved. If the particulate material is embedded in a suitable resin and then a surface ground and polished, a suitable surface for observation in the back-scattered mode is formed, and this produces ideal images at magnifications up to x5000 or higher for analysis by the above techniques. The particles will stand out as bright features in a dark background. An example is shown in Fig. 6A of a sample of Kaolin consolidated to 85 kPa; the direction of stressing is vertical in the micrograph. The corresponding images displaying the angular data and magnitudes using the 20,14 method are presented as Fig. 6B and 6C - the latter clearly

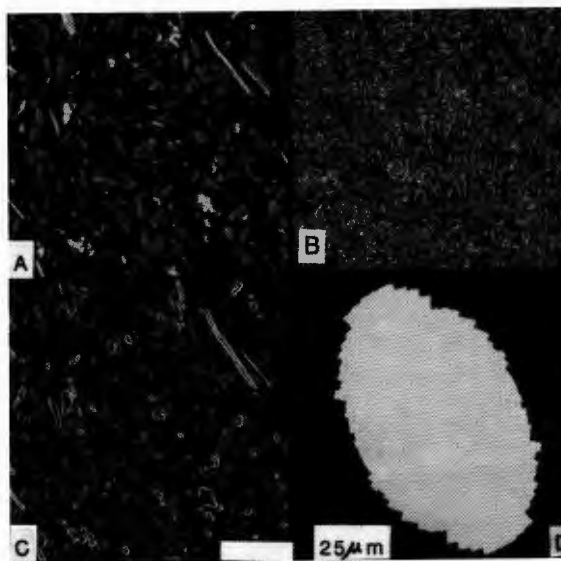


Fig. 6. Fig. 6A shows a back-scattered electron image of consolidated Kaolin. Fig. 6B - 6D are the associated angular information, magnitude information, and rosette diagram images.

showing the edges of the particles. The rosette diagram (Fig. 6D) clearly shows the preferred orientation direction. In this sample the index of anisotropy as determined by method (iii) is 0.348 while the mean length of the normalized resultant vector is 0.022.

Further Considerations

The selection of a particular *S,T* method will depend on circumstances. Smart and Tovey (1988) predicted that for noisy pictures, *S* should be large while the order of the solution of the intensity gradient should be kept low. Thus in such circumstances a 24,5 solution would be preferred to a 24,14 solution. Tovey et al (1989) used the image in Fig. 6A and two others of the same area, but taken with smaller apertures and hence produced more noisy images, to check this prediction. No recursive filtering was done on any image. In the above paper a few rosette diagrams were displayed to demonstrate this prediction, while in Table 1, a full set of the indices of anisotropy are shown for all *S,T* methods for the three images. The trends of the results generally confirm the prediction. The substantially increased noise with aperture 3 leads to much lower indices of anisotropy, although the methods with a large number of points but low order (24,5; 20,5, etc.) do produce results which are closest to the values for the larger apertures. If a 3 x 3 rank filter is passed over the noisy image before analysis then some improvement is noted as shown by the values in the final column. Most back-scattered images taken on the authors' instruments are taken with either of the two larger apertures, and thus the difference in index is usually small

TABLE 1. Indices of anisotropy determined for different analysis methods for three images taken with different final apertures.

Method	Aperture size			
	70 μ m	50 μ m	30 μ m	30 μ m*
4, 2	0.364	0.326	0.147	0.248
8, 5	0.341	0.324	0.153	0.245
12, 5	0.381	0.376	0.254	0.284
12, 9	0.348	0.300	0.130	0.186
20, 5	0.384	0.386	0.285	0.301
20,14	0.342	0.320	0.141	0.222
24, 5	0.379	0.380	0.281	0.308
24,14	0.334	0.314	0.178	0.233

* values obtained for image using 30 μ m aperture with a subsequent pass of a 3 x 3 rank filter during processing.

except where the array departs significantly from a circle (or square), and the order is high.

A further consideration is the contrast range in the original image. The following study was made. Fig. 7 shows four separate micrographs of the same area taken with differing amounts of contrast. Fig. 7A was an image taken with normal contrast (image 1) in the range 1 - 255 with just 1.19% of the pixels at saturation level. The mean intensity level is 128 while the standard deviation is 40. Fig. 7B was generated from 7A

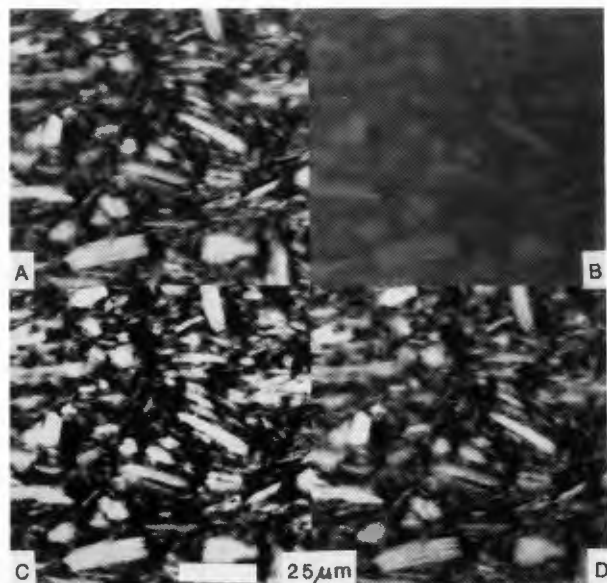


Fig. 7. Identical images taken with different contrast settings. Fig. 7A is the normal image; Fig. 7B with only 12.5% of normal contrast; Fig. 7C has double the normal contrast. Fig. 7D shows the effect of rescaling Fig. 7B back to the normal contrast range.

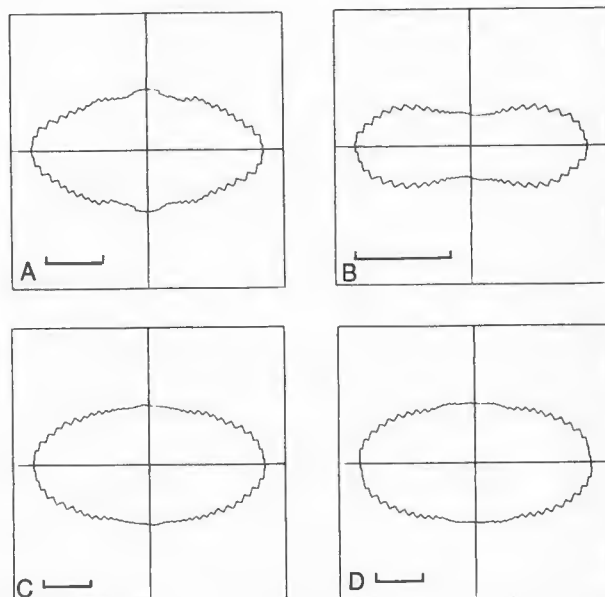


Fig. 8. The rosette diagrams for the corresponding images in Fig. 7. That in Fig. 8B is noticeably different from the others. Scale bar represents a length of 200 unit vectors.

by suppressing the contrast so that the mean was the same, but the standard deviation was now only 5 and the grey scale covered only 32 levels between 112 and 143. The resulting 'flat' image makes it difficult to see the features. Fig. 7C has the same mean but a standard deviation of 80 causing 11.03% of pixels to be at either saturation level. Fig. 7D was an attempt to recover the original image by rescaling the image in Fig. 7B. While the mean and standard deviations were the same as in Fig. 7a, only 32 levels between 0 and 255 are actually represented. Nevertheless, the image closely resembles Fig. 7A in appearance. The corresponding rosette diagrams using the 20,14 method are shown in Fig. 8, while the key data for several different S,T methods are shown in Table 2.

It appears that there is little difference between the diagrams for Figs. 8A, 8C, and 8D, but Fig. 8B is very different. A further study showed that provided that the contrast on the SEM was not less than half (or more than twice) that normally used, the index of anisotropy varied little. Where as in the case of Fig. 7B, the contrast was very low, an adequate representation can be achieved with the 20,14 method if the image is rescaled. It thus appears that contrast setting is not too critical, although arrays with larger numbers of points are to be preferred if the contrast departs substantially from the optimum setting.

The results for a single image for different S,T methods do show interesting trends. Generally, the more uniformly square (circular) the distribution the higher is the index of

Orientation Analysis of Micrographs

TABLE 2. Effects of contrast range on index of anisotropy

Method	Image number				
	1	2	3	4	5
4, 2	0.417	0.631	0.470	0.283	0.480
8, 5	0.529	0.794	0.519	0.415	0.394
12, 5	0.459	0.736	0.465	0.456	0.535
12, 9	0.419	0.609	0.482	0.423	0.660
20, 5	0.500	0.779	0.494	0.500	0.493
20,14	0.512	0.740	0.507	0.505	0.500
24, 5	0.519	0.813	0.509	0.520	0.481
24,14	0.547	0.788	0.537	0.541	0.497
	Contrast Settings				
mean	128	128	128	128	128
stdev	40	5	80	*40	160

* This image was reconstituted from image (3) by stretching the contrast.

anisotropy. It would seem that, contrary to the statements of Tovey and Smart (1986) where only a very approximate algorithm for the 8,5 method of analysis was used, the 12,9 method is less satisfactory than the 8,5 method.

While the examples in Figs. 6 and 7 were obtained from a mono-mineralic material, interesting results are obtained where there are a variety of minerals since, in general if back-scattered imaging is used, these minerals will appear as different brightnesses on the micrograph and a limited amount of image thresholding could be done to select only a certain mineral for analysis. In this way any differences in orientation between one mineral type and another may be studied.

Hitherto, the discussion has centered on the acquisition of planar images, and their analysis to provide information on fabric patterns. The analyses are clearly two dimensional, but the two dimensional orientation statistics may be combined with data from images taken on an orthogonal surface to obtain a three-dimensional estimate of orientation. Tovey and Sokolov (1981) showed that anisotropy data derived from two orthogonal surfaces could indeed be combined to correctly predict the likely anisotropy in the remaining orthogonal plane.

Conclusions

The intensity gradient technique provides a powerful method for orientation analysis in images, and is particularly useful in scanning electron microscope images where the mean brightness varies over the image. Little or no preliminary image processing is needed with this technique. While a little care must be taken in dealing with vectors of low magnitude, there are advantages over those techniques which involve some form of direct or adaptive thresholding, and as such are potentially of more applicability in fully automated systems. The general analysis now available permits filtering to be applied directly, and a choice can be made of the degree of precision with low order solutions favoured

for noisy pictures.

The effects of contrast variations do not appear to be that critical. Within a range from half to twice the normal contrast settings the indices of anisotropy and the rosette diagrams of orientations showed little difference. Noisy images, on the other hand are more troublesome and recursive filtering at the time of acquisition is recommended.

While the results from an image may be displayed assuming each vector at each pixel is treated equally, an alternative approach is to weight the vectors according to a function of their magnitude. Thus a direct weighting would automatically suppress the effects of vectors in regions of low contrast which may otherwise cause problems. Results may be conveniently displayed as rosette diagrams, or expressed as an index of anisotropy, or even as an equivalent resultant vector.

Orientation analysis and subsequent display of the results in a convenient form does require the interfacing of software with commercially available packages. The ease with which this can be done should be a major consideration when purchasing image analysis facilities.

Acknowledgements

The authors wish to acknowledge financial assistance from Scientific and Engineering Research Council Grant No. GRD/90574, and the Air Force Office for Support for Research (Grant (87-0346)). Research facilities at both the University of East Anglia and the University of Glasgow are also acknowledged.

References

- Curray JR (1956) The analysis of two dimensional orientation data. *Jour. Geol.* **64**, 117-131.
- Ehrlich R, Crabtree SJ, Kennedy SK, Cannon RL (1984) Petrographic image analysis, I. Analysis of Reservoir Pore Complexes. *J. Sedim. Petrol.*, **54**, 1365-1378.
- Ehrlich R, Crabtree SJ (1989) Determination of pore/throat relationships leads to successful physical modelling of porous media. In: *Proc. Int. Conf. on the Microstructure of Fine-grained Terrigenous marine sediments*, Bennett RH (ed), Springer-Verlag, Berlin, in press.
- Haralick RM (1984) Digital step edges from zero crossing of second directional derivatives. *IEEE Trans. Pattern Analysis and Machine Intelligence*, **6**, 58-68.
- Mardia KV (1972) *Statistics of Directional Data*. Academic Press, London, 357p.
- Marr D, Hildreth E (1980) Theory of edge detection. *Proc. Roy. Soc. London B.* **207**, 187-217.
- McConnachie I (1974) Fabric changes in consolidated Kaolin. *Geotechnique*, **24**, 207-222.
- Smart P (1966) Soil structure, mechanical properties and electron microscopy. PhD Thesis, Cambridge University, England.
- Smart P, Tovey NK (1982) *Electron microscopy of soils and sediments: Techniques*.

Oxford University Press, Oxford, xiii + 284p.

Smart P, Tovey NK (1988) Theoretical Aspects of Intensity Gradient Analysis. Scanning, 10, 115-121.

Tovey NK (1971) Soil Structure analysis using optical techniques on scanning electron micrographs. Scanning Electron Microsc., 1971: 49-56.

Tovey NK (1978) Potential developments in stereoscopic studies of sediments. In: Scanning Electron Microscopy in The Study of Sediments, Whalley WB (ed), Geoabstracts, Norwich, England, 105-117.

Tovey NK (1980) A digital computer technique for orientation analysis of micrographs of soil fabric. Jour. Microsc., 120, 303-317.

Tovey NK (1989) The microfabric of some Hong Kong marine soils. In: Proc. Int. Conf. on the Microstructure of Fine-grained Terrigenous marine sediments, Bennett RH (ed), Springer-Verlag, in press.

Tovey NK, Sokolov VN (1981) Quantitative SEM methods for soil fabric analysis. Scanning Electron Microsc., I; 536-554.

Tovey NK, Smart P (1986) Intensity gradient techniques for orientation analysis of electron micrographs. Scanning 8, 75-90.

Tovey NK, Smart P, Hounslow MW (1989) Quantitative Orientation Analysis of Soil Microfabric. In: Proc. 8th Int. Working Meeting Soil Micromorphology, Douglas LA (ed), Elsevier, Amsterdam, 1989. In press.

Unitt BM (1975) A digital computer method for revealing directional information in images. Jour. Phys. E. Scientific Instruments, 8, 423-425.

Unitt BM (1976) On-line digital image processing for the scanning electron microscope. PhD Thesis, Cambridge University, England.

Unitt BM, Smith KCA (1976) The application of the mini computer in scanning electron microscopy. In: Electron Microscopy, Proc. 6th European Congress on Electron Microscopy. Brandon DG (ed), TAL International Publishing Company, 1: 162-167.

Zhou YT, Venkateswar V, Chellappa R (1989) Edge detection and linear feature extraction using a 2-D random field model. IEEE Transactions on Pattern Analysis and Machine Intelligence, 11, 84-95.

Discussion with Reviewers

E Bisdom: SEMPER software is mainly used for image processing with a small section for image analysis. Because an image analyser is missing in the laboratory equipment, which can do orientation analysis on a routine basis, a more complicated system is advocated. The proposed system is important but should possibly be presented as one of a number of systems.

Authors: Orientation analyses using image analyses which are currently available requires some form of thresholding (which may not always be satisfactory) to obtain a binary image before analysis is possible, so losing potential image information. Further, only features above a given minimum size can be analysed in this way and problems often occur with touching particles which are not always satisfactorily dealt with. The general intensity gradient technique which is the main subject of this paper is not available on traditional image analysers and this paper thus describes a development for the future.

E Bisdom: Is it possible for the authors to look somewhat more into the future and pay less attention to what has been? The authors could, possibly, discuss some of the developments which improve SEM-SEMPER-image analyser connections.

Authors: The SEMPER image processing and analysis software is very flexible, covers all image analysis algorithms and is readily extendible for new algorithms such as those described in this paper. The ease with which this can be done is vitally important and was a major consideration in selecting such an image analysis system.

J. Fairing: The last sentence of the paper on software interfacing is of vital importance and cannot be stressed too strongly.

Authors: We concur: see also the reply to Dr. E. Bisdom above.